

Effects of walking speed and age on the muscle forces of unimpaired gait subjects

This content has been downloaded from IOPscience. Please scroll down to see the full text.

2016 J. Phys.: Conf. Ser. 705 012015

(<http://iopscience.iop.org/1742-6596/705/1/012015>)

View [the table of contents for this issue](#), or go to the [journal homepage](#) for more

Download details:

IP Address: 190.57.232.138

This content was downloaded on 10/05/2016 at 19:05

Please note that [terms and conditions apply](#).

Effects of walking speed and age on the muscle forces of unimpaired gait subjects

Carlos G. Fliger¹, Marcos J. Crespo², Ariel A. Braidot¹, Emiliano P. Ravera^{1,3}

¹Laboratory of Biomechanics, School of Engineering, National University of Entre Ríos, 3100, Argentina.

²Gait and Motion Analysis Laboratory, FLENI Institute for Neurological Research, B1625XAF, Argentina.

³National Council of Scientific and Technical Research (CONICET), Argentina.

E-mail: emilianoravera@bioingenieria.edu.ar

Abstract. Clinical gait analysis provides great contributions to the understanding of gait disorders and also provides a mean for a more comprehensive treatment plan. However, direct measures of muscle forces are difficult to obtain in clinical settings because it generally requires invasive techniques. Techniques of musculoskeletal modeling have been used for several decades to improve the benefits of clinical gait analysis, but many of the previous studies were focused on analyzing separately the muscle forces distribution of children or adult subjects with only one condition of walking speed. For these reason, the present study aims to enhance the current literature by describing the age and speed gait effects on muscle forces during walking.

We used a musculoskeletal model with 23 degrees of freedom and 92 musculotendon actuators to represent 76 muscles in the lower extremities and torso. The computed muscle control algorithm was used to estimate the muscle forces from the kinematics and to adjust the model obtained in the residual reduction algorithm.

We find that hamstrings has an important peak in the mid-stance phase in the adult group but this peak disappears in the children group with the same walking speed condition. Furthermore, the rectus femoris presents an increase in the muscle force during the pre- and mid-swing in concordance with the increment in the walking speed of subjects. This behavior could be associated with the role that the rectus femoris has in the acceleration of the knee joint. Finally, we show that the soleus is the muscle that perform the major force throughout the gait cycle regardless of age and walking speed.

1. Introduction

Clinical gait analysis provides great contributions to the understanding of gait disorders and also provides a mean for a more comprehensive treatment plan [1,2]. However, a complete distribution of dynamic muscle forces while walking is a challenge for many researchers [3,4]. Direct measures of muscle forces are difficult to obtain in clinical settings because it generally requires invasive techniques. Computational models that represent the human locomotor system are being currently proposed to sort out those limitations [3].

A musculoskeletal model represents a numeric set of anatomical parameters to quantify their interaction. Hence, the muscles are described as a simple line between patches of origin and insertion, while the joints are represented as fixed centers of rotation [5,6]. Estimation of muscle



forces using musculoskeletal models usually requires solving an optimization problem regardless of the method used to solve the equations that describe the dynamics musculoskeletal system, inverse or forward dynamics.

Techniques of musculoskeletal modeling have been used for several decades to improve the benefits of clinical gait analysis. Just in gait, *Seireg and Arvikar (1975)*, *Crowninshield et al. (1978)*, *Rohrer et al. (1984)* minimizing the sum of muscle forces to analyze the relationship between the net joints moments and muscle forces of the lower limb. *Patriarco et al. (1981)* found the muscle chemical-mechanical power, in addition to minimizing the muscle forces. *Crowninshield and Brand (1981)*, *Brand et al. (1986)*, *Glitsch and Baumann (1997)* and *Pedersen et al. (1997)* maximize the endurance by minimizing the muscle stress cubed [3]. Recent works like *van der Krogt et al. (2012)* [7] used the computed muscle control algorithm developed by *Thelen et al. (2003)* [8] to analyze the lower limb muscles weakness throughout the gait cycle in a group of adult subjects that walking at self-selected comfortable speed. *Ravera et al. (2014)* [9], developed a musculoskeletal model of the lower limb that simulate the smoothed EMG data through the sum of different Gaussian bells to analyze the muscle forces throughout the gait cycle in a group of children that walking at self-selected comfortable speed.

Many of the previous studies were focused on analyzing separately the muscle forces distribution on children or adults subjects, and generally in groups that walk at self-selected comfortable walking speed. For these reasons, the present study aims to enhance the current literature by describing speed gait effects on muscle forces of the lower limbs for a group of children and adult subjects that typically develop an unimpaired walking at three self-selected walking speeds. The aim of our study is to propose a single comprehensive source for muscle forces at a wide range of speeds and ages. We intend not to explain the underlying biomechanics of the speed and age variations, but rather to provide a thorough report of the data in a single source.

2. Methods

2.1. Participants

Two groups participated in this study (Table 1) to obtain a reliable data sample for a wide range of walking conditions. The first group included five children (7-14 years of age, 1.24-1.67 m in height and 22-53 kg in mass) that walk at a self-selected, comfortable walking speed. For operative reasons, the children were measured only once. The second group included eight adult subjects (23-42 years of age, 1.61-1.83 m in height and 63-83 kg in mass) that walk at three self-selected walking speeds (comfortable or free, slow and fast). After sufficient practice attempts, six successful trials were recorded for each speed condition. This resulted in a total of forty-eight trials per speed condition for the adults and ten trials for the children.

Walking speeds were rendered dimensionless using leg length (L_{leg}) following the scheme proposed by *Hof (1996)* [10]:

$$v^* = \frac{v}{\sqrt{gL_{leg}}} . \quad (1)$$

Both groups were examined by the Gait and Movement Laboratory at FLENI Institute for Neurological Research (Escobar, Argentina) team, and they exhibited normal gait patterns. This study was reviewed and approved by the research Ethics Committee. The protocol was explained to each subject, and either the participants or their caregivers signed informed consents.

Kinematic data were recorded using an Elite 2002 motion capture system (BTS Bioengineering, Italy) with 8 cameras (100Hz) and two force plates (Kistler 9281E, Kistler Group, Switzerland). Twenty-two retro-reflective skin markers were placed over bony landmarks (as indicated in the protocol of *Davis et al. (1991)* [11]). Electrical muscle activity data was recorded from the rectus femoris, semimembranosus, gastrocnemius and tibialis anterior muscle

Table 1: Subject characteristics and walking speeds.

Subject	Gender	Age (years)	Mass (Kg)	Leg length (m)	Slow speed (m/s) (non-dimensional)	Free Speed (m/s) (non-dimensional)	Fast speed (m/s) (non-dimensional)
Children							
1	F	11	40	0.79	-	1.32 (0.47)	-
2	M	14	53	0.89	-	0.98 (0.33)	-
3	F	7	22	0.65	-	1.45 (0.57)	-
4	F	8	38	0.69	-	1.34 (0.51)	-
5	F	9	30	0.72	-	1.02 (0.39)	-
Mean	-	9.80	36.60	0.75	-	1.27 (0.48)	-
SD	-	2.77	11.61	0.09	-	0.19 (0.09)	-
Adult							
1	M	28	78	0.95	1.04 (0.34)	1.27 (0.42)	1.55 (0.51)
2	M	42	79	0.95	1.08 (0.35)	1.11 (0.36)	1.80 (0.59)
3	M	29	75	0.94	0.93 (0.30)	1.37 (0.45)	1.44 (0.47)
4	M	27	64	0.86	0.93 (0.32)	1.08 (0.37)	1.15 (0.39)
5	F	30	63	0.81	0.92 (0.33)	1.12 (0.40)	1.55 (0.55)
6	M	29	83	1.00	1.01 (0.32)	0.99 (0.32)	1.03 (0.33)
7	F	23	68	0.92	0.58 (0.19)	1.09 (0.36)	1.24 (0.41)
8	M	27	77	0.91	0.94 (0.31)	1.06 (0.36)	1.34 (0.45)
Mean	-	29.37	73.37	0.92	0.93 (0.31)	1.14 (0.38)	1.39 (0.46)
SD	-	5.53	7.42	0.06	0.15 (0.05)	0.12 (0.04)	0.25 (0.08)

using a Teleemg surface dynamic electromyograph (BTS Bioengineering, Italy) with a sampling frequency of 2000 Hz [12].

2.2. Musculoskeletal Model

We used a musculoskeletal model, available in OpenSim (Fig. 1), with 23 degrees of freedom and 92 musculotendon actuators to represent 76 muscles in the lower extremities and torso. The degrees of freedom in this model included three translations and three rotations of the pelvis; three ball and socket joints, one located at the third lumbar vertebrae to model the interaction between pelvis and trunk and two at each hip joints; a custom joint with coupled translations and rotations at each knee; and a revolute joint at each ankle [13, 14].

OpenSim is an open-source platform for modeling, simulating, and analyzing the neuromusculoskeletal system. It includes low-level computational tools that allows one to derive equations of motion for dynamical systems, perform numerical integration, and solve constrained non-linear optimization problems. It offers access to control algorithms, actuators, and analyses; by integrating these components into a modeling and simulation platform [13].

In addition, SimTrack (one of the OpenSim tools) enables researchers to generate dynamic simulations of movement from motion capture data. This guides users through four steps to create a dynamic simulation: 1) a dynamic musculoskeletal model is scaled to match the anthropometry of an individual subject, 2) an inverse kinematics (IK) problem is solved, 3) a residual reduction algorithm (RRA) is applied and 4) the computed muscle control (CMC) is used to generate a set of muscle excitations.

Inverse kinematics and inverse dynamics, from the experimental marker trajectories and ground reaction forces, were used to calculate joint angles and moments. A dynamic simulation of one gait cycle was generated for each trial of each subject. The RRA was used to reduce residuals at the pelvis. This was proposed to minimize the effects of modeling and marker data processing errors that aggregate and lead to large nonphysical compensatory forces called residuals. Specifically, it altered the torso mass center of a subject-specific model and adjusted the kinematics of the model from inverse kinematics in order to be dynamically consistent with

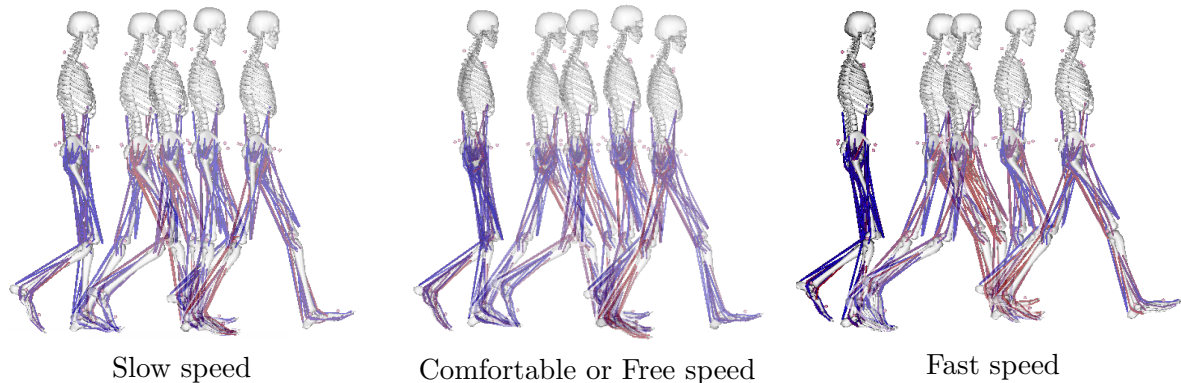


Figure 1: Musculoskeletal model used to generate three-dimensional simulations throughout the gait cycle. The musculotendon actuator colors indicate the level of activation on a scale from dark blue (no activation) to bright red (full activation).

the ground reaction force plate data. The CMC algorithm [8] was used to estimate the muscle forces from the kinematics and to adjust the model obtained in RRA. CMC used the static optimization approach along with feedforward and feedback controls to drive the kinematic trajectory of the musculoskeletal model toward a set of desired kinematics. In particular, the optimization criteria or cost function (2) was performed to be the sum of squared muscle activations [15, 16]:

$$J = \sum_{m=1}^{76} (a_m(t))^2, \quad (2)$$

where $a_m(t)$ is the steady-state activation of muscle m . All steps of our musculoskeletal simulations were implemented in concordance with the “best practices to verification and validation of musculoskeletal models” discussed by *Hicks et al. (2015)* [17].

3. Results

Figure 2 shows the mean and standard deviation of the sagittal, coronal, and transverse plane kinematics. It shows the same speed-related effects in the joint angles that were presented by *Schwartz et al. (2008)* [18]. In particular, we highlight a scaled nearly linear rise in hip flexion angle at initial contact and a plateau in ankle dorsiflexion angle of adult subject. Also, an increase in the plantarflexion angle, hip flexion angle and hip rotation angle was found in children throughout the gait cycle in contrast with adult subjects.

The mean and standard deviation of net joint moments of hip, knee and ankle are shown in Figure 3. Similar morphological patterns are found in both age groups, in particular a slight rise was found in the joint moment peaks when adult subjects increase their walking speed. Abduction/adduction hip joint moments present two main peaks at 10% and 50% of the gait cycle respectively. Only the first peak shows a significant increase when the subjects walk faster.

Prior to analyzing the results of the musculoskeletal simulations for each participant through OpenSim, we compared the muscle activations from CMC with the EMG signals recorded for each individual trial, which were qualitatively similar (i.e. present their peaks in same areas of the gait cycle and are morphologically similar), as shown in Figure 4.

Although the simulations performed in OpenSim include a complete set of lower limb muscles, as was described in section 2.2, for the later analysis we have considered the behaviors of the Gluteus Maximus (GM), Gluteus Medius (Gm), Hamstrings (Ham), Vastus (Vas), Rectus Femoris (RF), Gastrocnemius (Gas), Soleus (Sol) and Tibialis Anterior (TA) as the most

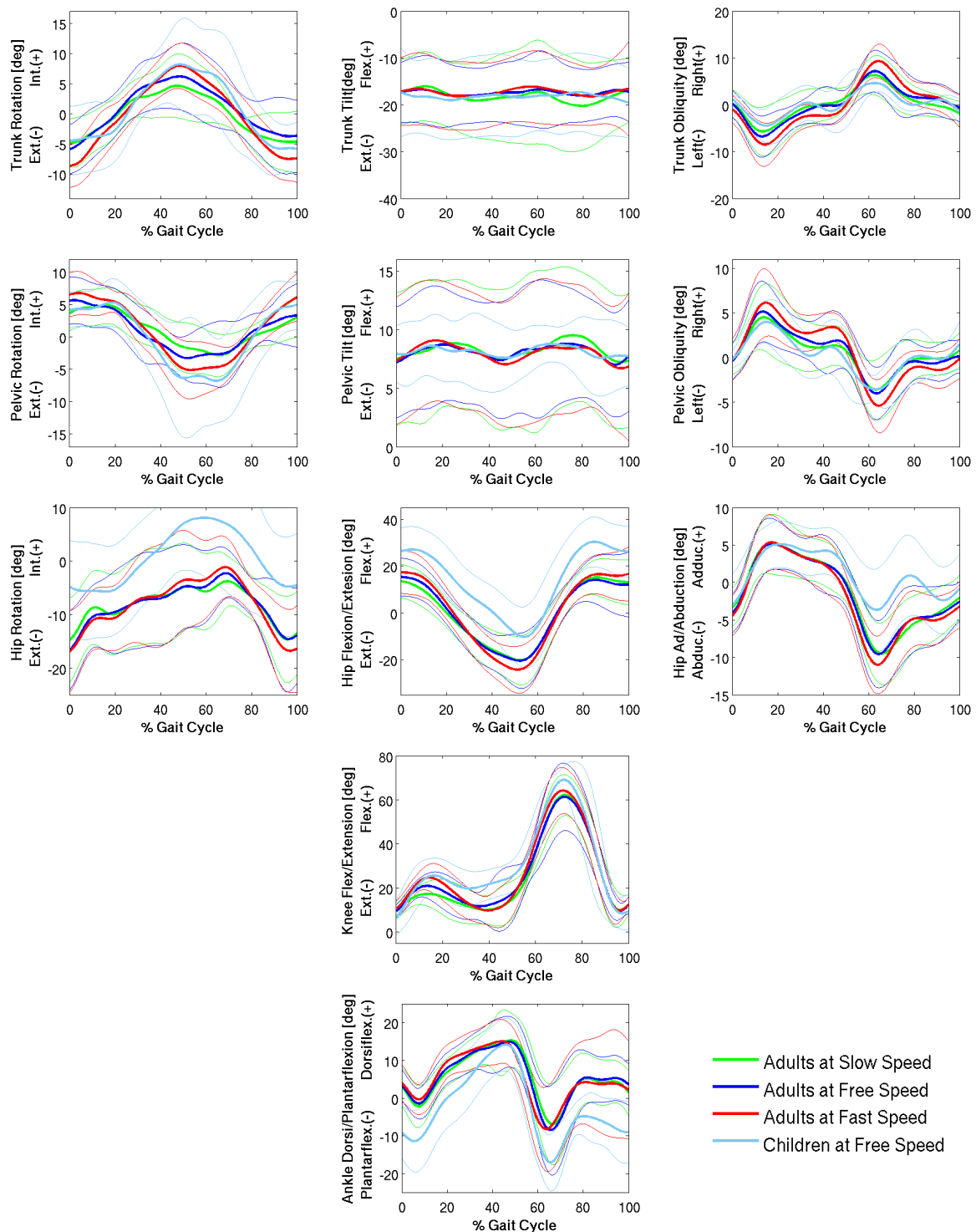


Figure 2: Joint angles for children and adult groups across walking speed. Each bold line represents the average of trials and the thin lines represent the standard deviation of trials within the corresponding group.

representative muscle groups in vertical and fore-aft accelerations during gait [19].

Muscle forces estimated by CMC algorithm are shown in Figure 5. Hamstrings has an

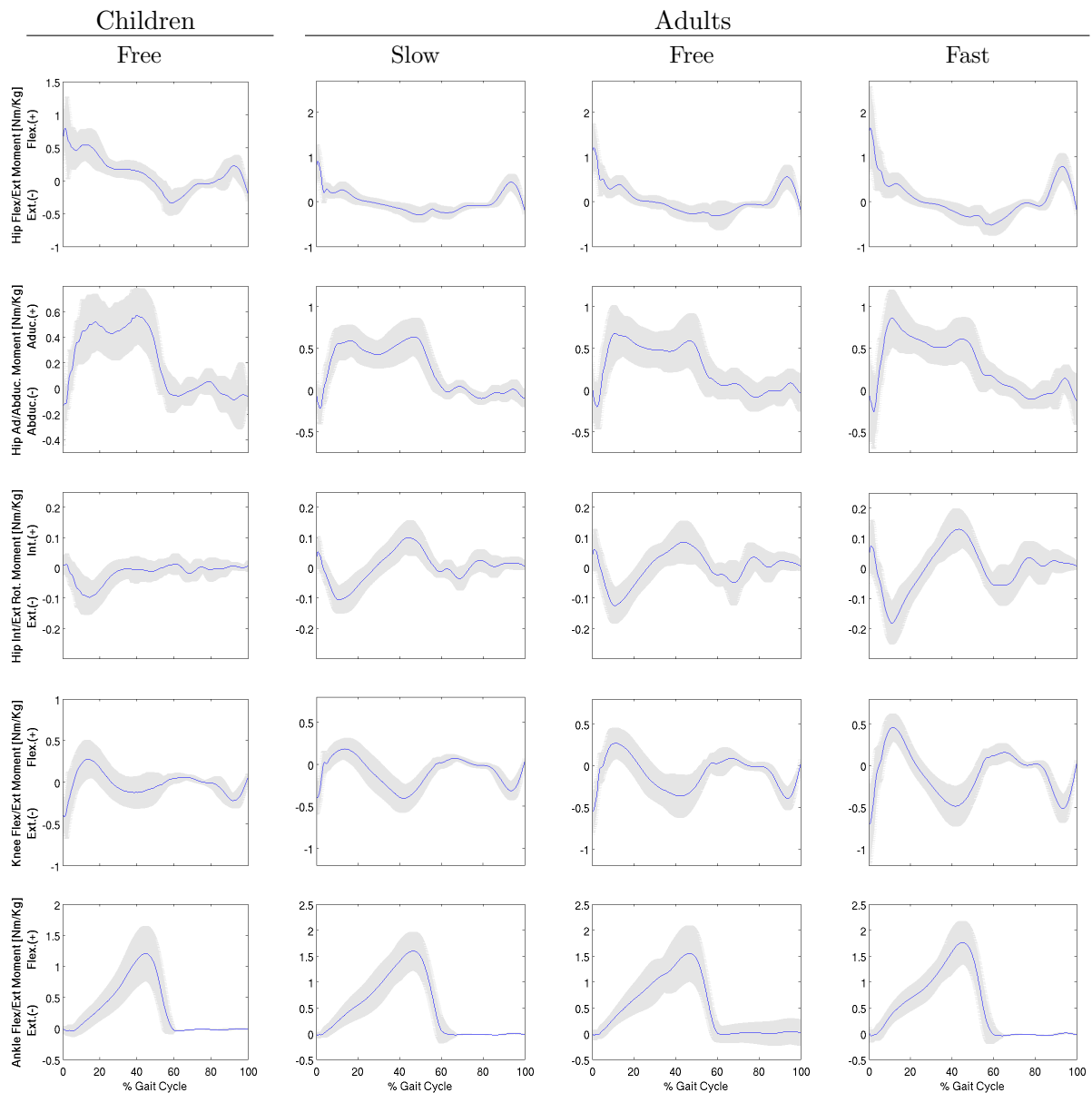


Figure 3: Mean (blue lines) and standard deviation (shaded area) of the joint moments for children that walking at self-selected comfortable speed, and adults that walking at three self-selected speeds (slow, comfortable or free and fast).

important peak in the mid-stance phase in the adult group but this peak disappears in the children group with the same walking speed condition. Furthermore, the rectus femoris presents an increase in the muscle force during the pre- and mid-swing in concordance with the increment in the walking speed of subjects. This behavior could be associated with the role that the rectus femoris has in the acceleration of the knee joint [20]. In addition, in the children group the gluteus maximus has a great peak of muscle force during mid-stance, whereas the same peak is only showed weakly in adults. On the other hand, the gastrocnemius, soleus and tibialis anterior present their main variations in the stance phase, in accordance with the role that they have in the plantar/dorsiflexion joint moment [21,22]. In particular, we show that tibialis anterior has a marked peak in the initial contact of the gait cycle in accordance with the dorsiflexion peak

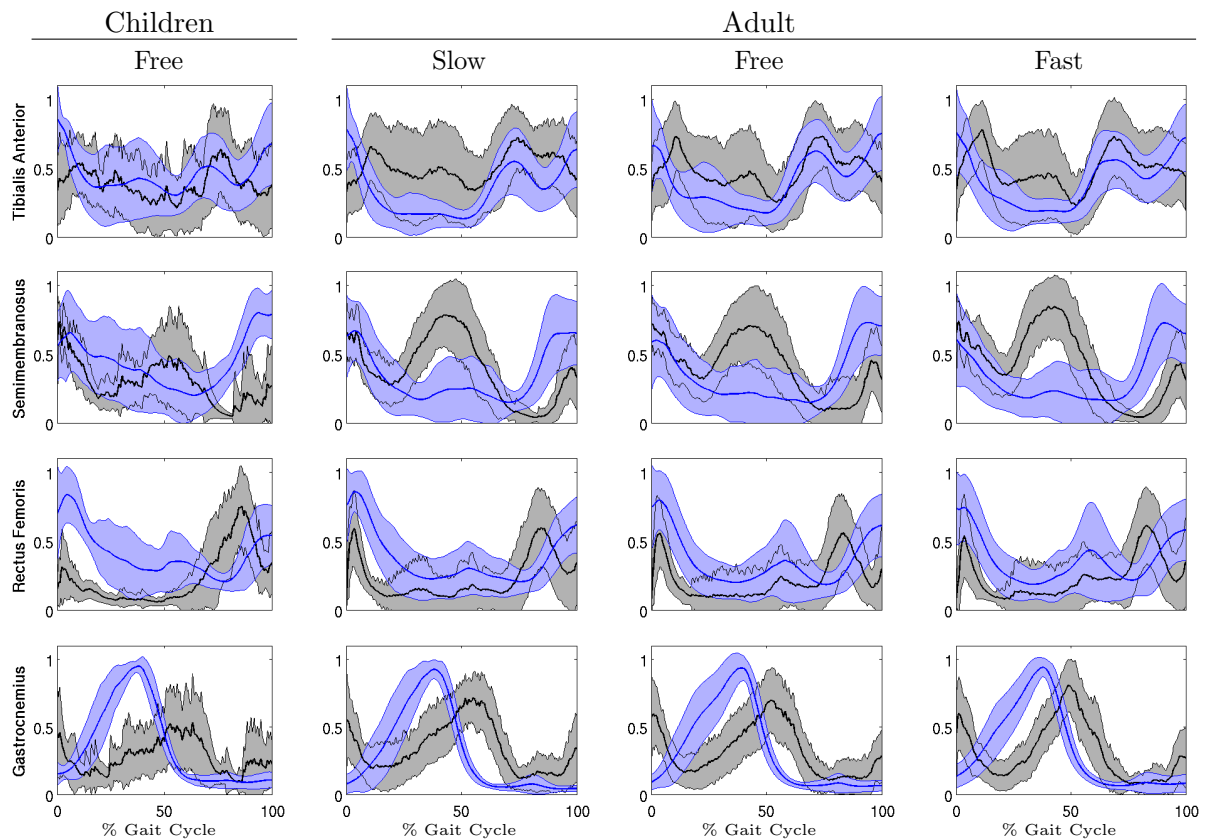


Figure 4: Mean simulated muscle activations (black lines) and mean experimental EMG (blue lines) throughout the gait cycle for children that walking at a comfortable (or free) self-selected speed and adults that walking at three self-selected speeds (slow, free and fast) for all four muscles for which EMG was collected. Shaded areas show the standard deviations. Experimental EMG data are rectified and bi-directionally low-pass filtered at 6 Hz. All signals were normalized by their peak value.

of ankle joint moment (see Fig. 3) and this muscle force peak appears to increase with walking speed. Finally, the gastrocnemius and soleus present their peaks at the end of stance phase by acting in antagonistic form with tibialis anterior.

In the end, Figure 6 shows the average values over the gait cycle of the mean and standard deviation of each muscle force in order to find which muscles perform more force throughout the gait cycle. Hence, we conclude that the soleus is the muscle that provides the major force during walk in concordance with the study of *Zajac (2002)* [22], and the gluteus maximus (a big muscle) is the muscle that provides the smaller force throughout the gait cycle.

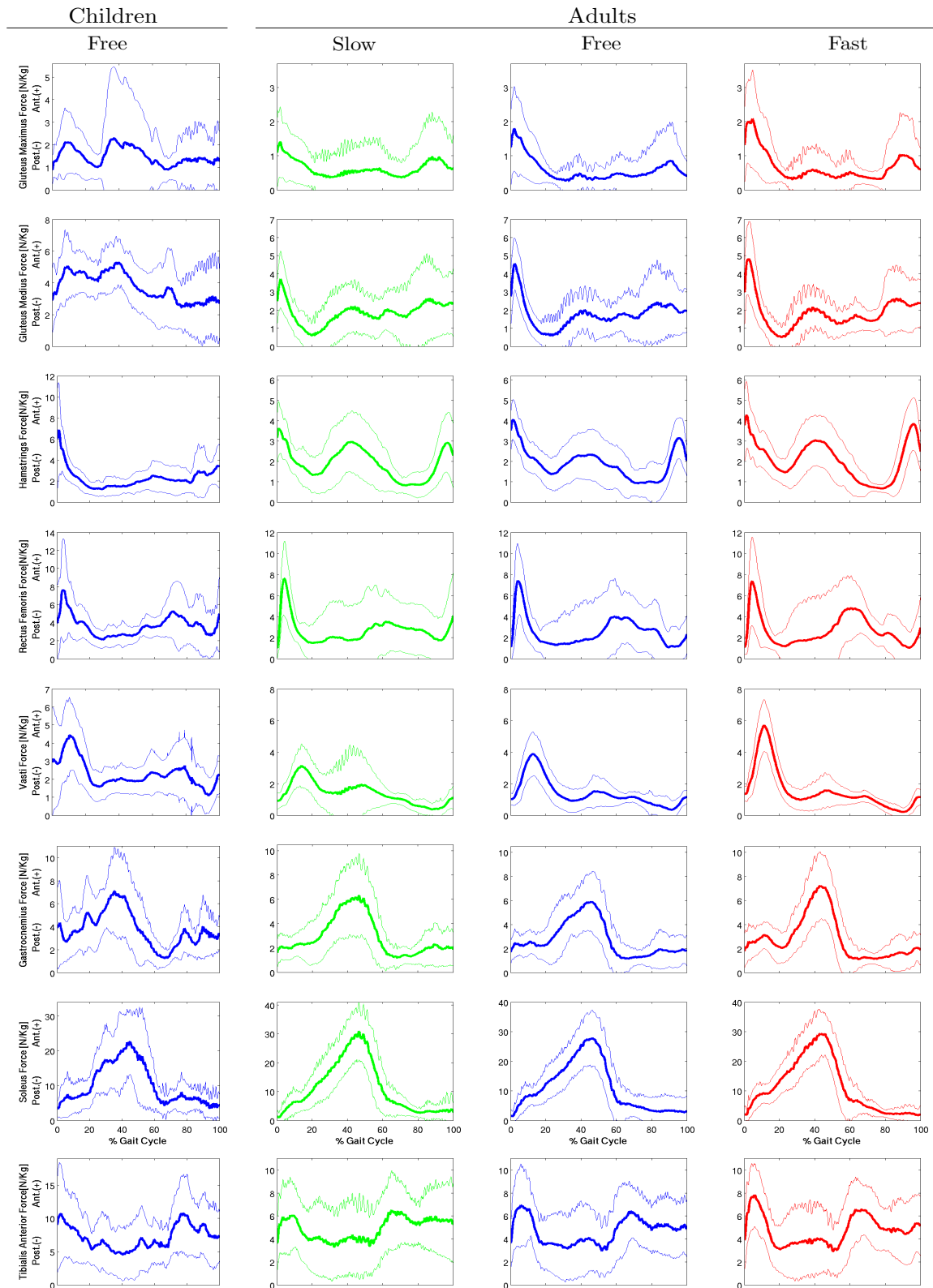


Figure 5: Mean (bold line) and standard deviation (thin lines) of muscle forces for children that walk at a comfortable self-selected walking speed and adults that walk at three self-selected walking speeds (slow, comfortable or free and fast).

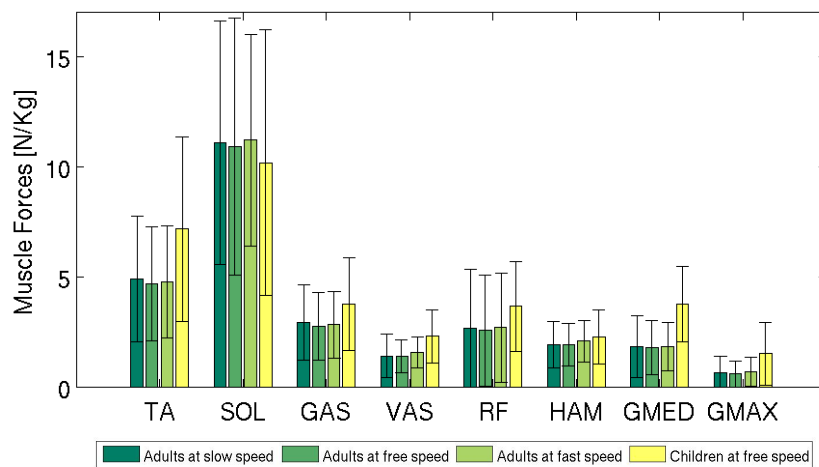


Figure 6: Average values over the gait cycle of the mean and standard deviation of muscle forces for children that walk at self-selected comfortable walking speed and adults that walk at three self-selected walking speeds (slow, comfortable or free and fast).

4. Discussion

Techniques of musculoskeletal modeling have been used by several decades to improve the benefits of clinical gait analysis, but many of the previous studies were focused on analyzing separately the muscle forces distribution of children or adult subjects with only one condition of walking speed. For these reason, the present study aims to enhance the current literature by describing speed gait effects on muscle forces of the lower limbs for a group of children and adult subjects that typically develop an unimpaired gait at three self-selected walking speeds.

When analyzing the hip flexion/extension moment joint (Fig. 3), it appears to be modulated by the action of rectus femoris, gluteus maximus, gluteus medialis and hamstrings mainly during the initial contact. However, from the mid-stance until the end of swing, this net joint moment tends to zero while the antagonistic activity of hamstrings and rectus femoris is shown to rise. In the abduction/adduction hip joint moment, the gluteus medialis produces an abduction moment while the gluteus maximus and hamstrings perform an adduction moment. The decrease in abduction joint moment during the mid-stance happens followed by a modulation of gluteus medialis and hamstrings.

On the other hand, the knee extensor joint moment in mid-stance (Fig. 3) occurs because an activation of the gastrocnemius together with the hamstrings muscles (Fig. 5). Its behavior produces a force peak at the end of swing phase that coincides with the peak present in the hamstrings force. Also, when the minimum value of knee flexion joint moment occurs, around the pre-swing or initial swing, an increase in the muscle forces of vastus and rectus femoris was found; they appear to be the main responsables of the second knee net flexion joint moment.

Finally, the ankle flexion/extension net joint moment is produced mainly by the soleus and the gastrocnemius while the tibiales anterior acts modulating the net joint moment behavior (Fig. 5). In addition, the soleus is the muscle that perform the major force throughout the gait cycle regardless of age and walking speed.

Acknowledgments

The authors thank the FLENI Institute for Neurological Research for providing data from healthy subjects and the National Council of Scientific and Technical Research (CONICET) and PICTO 222-2009 (AGENCIA) for providing the funds needed for this research.

References

- [1] Wren T a L, Otsuka N Y, Bowen R E, Scaduto A a, Chan L S, Sheng M, Hara R and Kay R M 2011 *Gait & Posture* **34** 364–9 ISSN 1879-2219 URL <http://www.ncbi.nlm.nih.gov/pubmed/21723131>
- [2] de Morais Filho M C, Kawamura C M, dos Santos C A and Mattar R 2012 *Gait & Posture* **36** 201–4 ISSN 1879-2219 URL <http://www.ncbi.nlm.nih.gov/pubmed/22425638>
- [3] Erdemir A, McLean S, Herzog W and van den Bogert A J 2007 *Clinical Biomechanics (Bristol, Avon)* **22** 131–54 ISSN 0268-0033 URL <http://www.ncbi.nlm.nih.gov/pubmed/17070969>
- [4] Amarantini D, Rao G and Berton E 2010 *Journal of Biomechanics* **43** 1827–30 ISSN 1873-2380 URL <http://www.ncbi.nlm.nih.gov/pubmed/20206935>
- [5] Kaufman K R, An K N W, Litchy W J and Chao E Y 1991 *Neuroscience* **40** 781–92 ISSN 0306-4522 URL <http://www.ncbi.nlm.nih.gov/pubmed/2062441>
- [6] Arnold E M, Ward S R, Lieber R L and Delp S L 2010 *Annals of Biomedical Engineering* **38** 269–79 ISSN 1521-6047 URL <http://www.ncbi.nlm.nih.gov/pubmed/19957039>
- [7] van der Krogt M M, Delp S L and Schwartz M H 2012 *Gait & Posture* **36** 113–9 ISSN 1879-2219 URL <http://www.ncbi.nlm.nih.gov/pubmed/22386624>
- [8] Thelen D G, Anderson F C and Delp S L 2003 *Journal of Biomechanics* **36** 321–328 ISSN 00219290 URL <http://www.ncbi.nlm.nih.gov/pubmed/12594980>
- [9] Ravera E P, Crespo M J and Braidot A A A 2014 *Computer Methods in Biomechanics and Biomedical Engineering* 1–12 ISSN 1476-8259 URL <http://www.ncbi.nlm.nih.gov/pubmed/25408069>
- [10] Hof A 1996 *Gait & Posture* **4** 222–3
URL <http://www.sciencedirect.com/science/article/pii/0966636295010572>
- [11] Davis R B, Öunpuu S, Tyburski D and Gage J R 1991 *Human Movement Science* **10** 575–587 ISSN 01679457
URL <http://www.sciencedirect.com/science/article/pii/016794579190046Z>
- [12] Stegeman D F and Hermens H J 1999 Standards for surface electromyography: the European project "Surface EMG for non-invasive assessment of muscles (SENIAM) Tech. rep. URL www.seniam.org
- [13] Delp S L, Anderson F C, Arnold A S, Loan P, Habib A, John C T, Guendelman E and Thelen D G 2007 *IEEE Transactions on Bio-medical Engineering* **54** 1940–50 ISSN 0018-9294 URL <http://www.ncbi.nlm.nih.gov/pubmed/18018689>
- [14] Anderson F C and Pandy M G 1999 *Computer Methods in Biomechanics and Biomedical Engineering* **2** 201–231 ISSN 1476-8259 URL <http://www.ncbi.nlm.nih.gov/pubmed/11264828>
- [15] Anderson F C and Pandy M G 2001 *Journal of Biomechanics* **34** 153–61 ISSN 0021-9290 URL <http://www.ncbi.nlm.nih.gov/pubmed/11165278>
- [16] Thelen D G and Anderson F C 2006 *Journal of Biomechanics* **39** 1107–15 ISSN 0021-9290 URL <http://www.ncbi.nlm.nih.gov/pubmed/16023125>
- [17] Hicks J L, Uchida T K, Seth A, Rajagopal A and Delp S 2015 *Journal of Biomechanical Engineering* **137** 1–24 ISSN 0148-0731 URL <http://www.ncbi.nlm.nih.gov/pubmed/25474098>
- [18] Schwartz M H, Rozumalski A and Trost J P 2008 *Journal of Biomechanics* **41** 1639–50 ISSN 0021-9290 URL <http://www.ncbi.nlm.nih.gov/pubmed/18466909>
- [19] Liu M Q, Anderson F C, Pandy M G and Delp S L 2006 *Journal of Biomechanics* **39** 2623–30 ISSN 0021-9290
URL <http://www.ncbi.nlm.nih.gov/pubmed/16216251>
- [20] Arnold E M, Hamner S R, Seth A, Millard M and Delp S L 2013 *The Journal of Experimental Biology* **216** 2150–60 ISSN 1477-9145 URL <http://www.ncbi.nlm.nih.gov/pubmed/23470656>
- [21] Neptune R R, Kautz S a and Zajac F E 2001 *Journal of Biomechanics* **34** 1387–98 ISSN 0021-9290 URL <http://www.ncbi.nlm.nih.gov/pubmed/11672713>
- [22] Zajac F E, Neptune R R and Kautz S a 2002 *Gait & Posture* **16** 215–32 ISSN 0966-6362 URL <http://www.ncbi.nlm.nih.gov/pubmed/12443946>